

# Photoproduction of Prompt $J/\psi$ in Association with a $c\bar{c}$ Pair within the Framework of Non-relativistic QCD at the International Linear Collider

Zhan Sun<sup>\*</sup> and Xing-Gang Wu<sup>†</sup>

*Department of Physics, Chongqing University, Chongqing 401331, P.R. China and  
Institute of Theoretical Physics, Chongqing University, Chongqing 401331, P.R. China*

Hong-Fei Zhang<sup>‡</sup>

*Department of Physics, School of Biomedical Engineering,  
Third Military Medical University, Chongqing 400038, P.R. China and  
Chongqing University of Posts & Telecommunications, Chongqing, 400065, P.R. China  
(Dated: June 12, 2019)*

We present a systematical study on the photoproduction of prompt  $J/\psi$  in association with a  $c\bar{c}$  pair within the framework of non-relativistic QCD at the future high-energy  $e^+e^-$  collider - International Linear Collider, including both direct and feed-down contributions. For direct  $J/\psi$  production, the states with color-octet  $c\bar{c}$ -components, especially  $|c\bar{c}[^3P_J^{[8]}]g\rangle$  and  $|c\bar{c}[^1S_0^{[8]}]g\rangle$ , provide dominant contribution to the production cross-section, which are about sixty times over that of the color-singlet state  $|c\bar{c}[^3S_1^{[1]}]\rangle$ . This is clearly shown by the transverse momentum ( $p_t$ ) and rapidity distributions. The feed-down contribution from  $\psi'$  and  $\chi_{cJ}$  ( $J = 0, 1, 2$ ) is sizable, which is  $\sim 20\%$  to the total prompt cross-section. Besides the yields, we also calculate the  $J/\psi$  polarization parameter  $\lambda$ . In small  $p_t$  region, the polarization of the prompt  $J/\psi$  is longitudinal due to  $|c\bar{c}[^3P_J^{[8]}]g\rangle$ , which becomes transverse in high  $p_t$  region due to  $|c\bar{c}[^3S_1^{[8]}]gg\rangle$ . Thus the  $J/\psi$  photoproduction shall provide a useful platform for testing the color-octet mechanism.

PACS numbers: 13.66.Bc, 12.39.Jh, 14.40.Pq, 12.38.Bx

## I. INTRODUCTION

With its heavy mass  $m$  the heavy quark ( $Q$ ) will move with a small velocity  $v_Q$  inside a heavy quarkonium. This results in a hierarchy of energy scales,  $m \gg mv_Q \gg mv_Q^2$ , and the dynamics at different energy scales is different. The non-relativistic QCD (NRQCD) provides a systematical way to separate the effects from the dynamics at different energy scales [1]. A comprehensive review of its application to quarkonium physics can be found in Refs. [2, 3]. The heavy quarkonium can be expanded as a Fock-state expansion, the dominant one is of course  $|Q\bar{Q}\rangle$ , and it also contains the higher-Fock states as  $|Q\bar{Q}g\rangle$  and etc., which includes dynamical gluon(s) or light quark(s). Although the probabilities of finding higher-Fock states are suppressed by certain powers of  $v_Q$ , their effects can be very significant [4–6]. By taking the color-octet Fock states into account, the Tevatron data on  $\psi'$ -anomaly can be explained [4]. Using the newly fitted color-octet long distance matrix elements (LDMEs) [7, 8], the LHCb and CMS data of the  $\eta_c$  and  $J/\psi$  hadroproductions [9–11], including the  $J/\psi$  polarization data, can be consistently reproduced.

Despite many successes, the NRQCD still faces some challenges. As an important example, the Belle and the LHCb collaborations [12, 13] have measured the  $J/\psi$  production associated with a  $c\bar{c}$  pair, which however show

large discrepancies from the NRQCD predictions [14–21]. For example, the predicted angular distribution of  $J/\psi$  is different from the Belle data, and the predicted  $J/\psi$  production cross-section is lower than the LHCb data by about one order of magnitude. Thus it is helpful to find another platform to test NRQCD.

A detailed prediction for  $J/\psi$  production associated with a  $c\bar{c}$  pair at the super- $Z$  factory has been done in Ref.[22]. Due to  $Z^0$ -boson resonance effect, sizable  $J/\psi$  events can be achieved there. The proposed International Linear Collider (ILC) [23] is another useful  $e^+e^-$  collider, which has been designed to run at a high collision energy from several hundred GeV to TeV together with a high luminosity about  $\mathcal{L} \simeq 10^{34}\text{cm}^{-2}\text{s}^{-1}$ . In the paper, we will present a systematic NRQCD prediction on the photoproduction of prompt  $J/\psi$  with a  $c\bar{c}$  pair, including both direct and feed-down contributions.

Following the standard velocity-scaling rule [1], the physical state of  $J/\psi$  can be expanded as

$$J/\psi = \mathcal{O}(1)|c\bar{c}[^3S_1^{[1]}]\rangle + \mathcal{O}(v_c)|c\bar{c}[^3P_J^{[8]}]g\rangle + \mathcal{O}(v_c^2)|c\bar{c}[^3S_1^{[8]}]gg\rangle + \mathcal{O}(v_c^2)|c\bar{c}[^1S_0^{[8]}]g\rangle + \cdots, (1)$$

where  $J = (0, 1, 2)$ . In the following, to short the notations, we shall adopt  $J/\psi(^3S_1^{[1]})$  to stand for the Fock-state  $|c\bar{c}[^3S_1^{[1]}]\rangle$ ,  $J/\psi(^3P_J^{[8]})$  to stand for the Fock-state  $|c\bar{c}[^3P_J^{[8]}]g\rangle$ , and so on so forth. For the direct  $J/\psi$  production, we shall consider the contributions from all important Fock states,  $J/\psi(^3S_1^{[1]})$ ,  $J/\psi(^1S_0^{[8]})$ ,  $J/\psi(^3S_1^{[8]})$  and  $J/\psi(^3P_J^{[8]})$ . The feed-down contributions from high excited charmonium states  $\psi'$  and  $\chi_{cJ}$  shall also be con-

<sup>\*</sup> zhansun@cqu.edu.cn

<sup>†</sup> wuxg@cqu.edu.cn

<sup>‡</sup> hfzhang@ihep.ac.cn

sidered, since they may decay to  $J/\psi$  via electroweak or strong radiations with high probability and provide sizable contributions to the final  $J/\psi$  events. The  $\psi'$  production can be obtained from that of  $J/\psi$  by directly replacing  $J/\psi$  LDMEs to  $\psi'$  ones. As for  $\chi_{cJ}$  productions, in addition to its direct production for which the  $\chi_{cJ}(^3P_J^{[1]})$  and  $\chi_{cJ}(^3S_1^{[8]})$  are involved, its feed-down contribution from  $\psi'$  shall also be calculated.

The remaining parts of the paper are organized as follows. In Sec.II, we describe the calculation technology for treating the  $J/\psi$  production in association with a  $c\bar{c}$ -pair. The input parameters are also introduced there. In Sec.III, we give the predictions for the yields and polarizations of  $J/\psi$  at the ILC. The last section is reserved for a summary.

## II. CALCULATION TECHNOLOGY AND INPUT PARAMETERS

At the ILC, the charmonium  $H$  can be produced via the process,  $e^+ + e^- \rightarrow e^+ + e^- + H(c\bar{c}) + c + \bar{c}$ . For the photoproduction via the process,  $\gamma\gamma \rightarrow H(c\bar{c}) + c + \bar{c}$ , the photons may interact either directly (direct photon production) or indirectly via their hadronic components (resolved photon production) with the quarks or antiquarks. In the paper we shall focus our attention on leading contribution from the direction photon production. The differential cross-section for the charmonium  $H$  can be factorized as

$$d\sigma^H = \sum_n \int dx_1 dx_2 f_\gamma(x_1) f_\gamma(x_2) \times d\hat{\sigma}(\gamma\gamma \rightarrow c\bar{c}[n] + c + \bar{c}) \langle \mathcal{O}^H(n) \rangle. \quad (2)$$

$\hat{\sigma}$  stands for short-distance cross-section, representing the production of an intermediate perturbative state  $(c\bar{c})[n]$  with quantum number  $n$ .  $\langle \mathcal{O}^H(n) \rangle$  is non-perturbative but universal LDMEs, which is proportional to the inclusive transition probability of the perturbative state  $(c\bar{c})[n]$  into the bound-state.  $f_\gamma(x)$  is the photon density function with  $x$  being the momentum fraction of the photon to the initial electron or positron.

For the hard subprocess  $\gamma\gamma \rightarrow c\bar{c}[n] + c + \bar{c}$ , there are totally 20 diagrams for  $[n] = ^3S_1^{[1]}$  and  $[n] = ^3P_J^{[1]}$ , 32 diagrams for  $[n] = ^3S_1^{[8]}$ , and 28 diagrams for  $[n] = ^1S_0^{[8]}$  and  $[n] = ^3P_J^{[8]}$ . Typical Feynman diagrams are presented in Fig.(1). Those Feynman diagrams can be generated and the corresponding short-distance cross-sections can be calculated by using the well-established FDC package. The FDC is a general-purpose program for Feynman diagram calculation which realizes an automatic deduction from physical models to final numerical results for lower-order processes [25].

At the high-energy  $e^+e^-$  collider such as ILC, the laser backscattering (LBS) from the incident electron and positron beams leads to high luminosity photon beams [26]. Those LBS photons are hard enough and

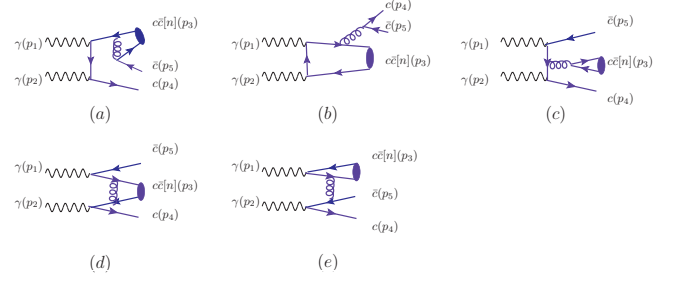


FIG. 1. Typical Feynman Diagrams for the hard subprocess  $\gamma(p_1)\gamma(p_2) \rightarrow c\bar{c}[n](p_3) + c(p_4) + \bar{c}(p_5)$ , in which (a, d) are for color-singlet states, (a, b, c, d) are for  $c\bar{c}[^3S_1^{[8]}]$  and (a, d, e) are for  $c\bar{c}[^1S_0^{[8]}]$  and  $c\bar{c}[^3P_J^{[8]}]$ , respectively.

carry a large fraction of the energy of the incident lepton beams. Moreover, as pointed out by Refs. [27–29], using LBS photons the  $\gamma\gamma$  collisions can approximately achieve the same high luminosity as that of the  $e^+e^-$  beams. Thus, we adopt the LBS density function to do our calculation [26]

$$f_\gamma(x) = \frac{1}{N} \left[ 1 - x + \frac{1}{1-x} - 4r(1-r) \right], \quad (3)$$

where  $r = x/[x_m(1-x)]$  and the normalization factor

$$N = \left( 1 - \frac{4}{x_m} - \frac{8}{x_m^2} \right) \log \chi + \frac{1}{2} + \frac{8}{x_m} - \frac{1}{2\chi^2}. \quad (4)$$

Here  $\chi = 1 + x_m$ ,  $x_m \simeq 4.83$  [30] and the LBS photon energy is restricted by  $0 \leq x \leq x_m/(1+x_m) = 0.83$ .

The unpolarized differential cross-section of prompt  $J/\psi$  is obtained by adding the unpolarized cross-sections of the various direct-production processes multiplied by appropriate branching fractions, i.e.

$$d\sigma^{\text{prompt } J/\psi} = d\sigma^{J/\psi} + \sum_J \mathcal{B}r(\chi_{cJ} \rightarrow J/\psi + \gamma) d\sigma^{\chi_{cJ}} + \sum_J \mathcal{B}r(\psi' \rightarrow \chi_{cJ} + \gamma) \mathcal{B}r(\chi_{cJ} \rightarrow J/\psi + \gamma) d\sigma^{\psi'} + \mathcal{B}r(\psi' \rightarrow J/\psi + X) d\sigma^{\psi'}. \quad (5)$$

As for the branching ratios, we take [31]

$$\mathcal{B}r(\psi' \rightarrow J/\psi + X) = 60.9 \times 10^{-2}, \quad (6)$$

$$\mathcal{B}r(\psi' \rightarrow \chi_{c0} + \gamma) = 9.99 \times 10^{-2}, \quad (7)$$

$$\mathcal{B}r(\psi' \rightarrow \chi_{c1} + \gamma) = 9.55 \times 10^{-2}, \quad (8)$$

$$\mathcal{B}r(\psi' \rightarrow \chi_{c2} + \gamma) = 9.11 \times 10^{-2}, \quad (9)$$

$$\mathcal{B}r(\chi_{c0} \rightarrow J/\psi + \gamma) = 1.27 \times 10^{-2}, \quad (10)$$

$$\mathcal{B}r(\chi_{c1} \rightarrow J/\psi + \gamma) = 33.9 \times 10^{-2}, \quad (11)$$

$$\mathcal{B}r(\chi_{c2} \rightarrow J/\psi + \gamma) = 19.2 \times 10^{-2}. \quad (12)$$

As for the LDMEs, we take [7, 8, 32]:

$$\langle O^{\chi_{cJ}}(^3S_1^{[8]}) \rangle = (2J+1) \times 2.15 \times 10^{-3} \text{ GeV}^3, \quad (13)$$

$$\langle O^{\chi_{cJ}}(^3P_J^{[1]}) \rangle = (2J+1) \times \frac{3}{4\pi} |R'_{1P}(0)|^2, \quad (14)$$

$$\langle O^{\psi'}(^1S_0^{[8]}) \rangle = 1.0 \times 10^{-2} \text{ GeV}^3, \quad (15)$$

$$\langle O^{\psi'}(^3S_1^{[8]}) \rangle = 0.401 \times 10^{-2} \text{ GeV}^3, \quad (16)$$

$$\frac{\langle O^{\psi'}(^3P_0^{[8]}) \rangle}{m_c^2} = 0.682 \times 10^{-2} \text{ GeV}^3, \quad (17)$$

$$\langle O^{\psi'}(^3S_1^{[1]}) \rangle = \frac{1}{4\pi} |R_{2S}(0)|^2, \quad (18)$$

$$\langle O^{J/\psi}(^3S_1^{[1]}) \rangle = 0.556 \text{ GeV}^3, \quad (19)$$

$$\langle O^{J/\psi}(^1S_0^{[8]}) \rangle = 0.780 \times 10^{-2} \text{ GeV}^3, \quad (20)$$

$$\langle O^{J/\psi}(^3S_1^{[8]}) \rangle = 1.057 \times 10^{-2} \text{ GeV}^3, \quad (21)$$

$$\frac{\langle O^{J/\psi}(^3P_0^{[8]}) \rangle}{m_c^2} = 1.934 \times 10^{-2} \text{ GeV}^3, \quad (22)$$

where  $J = (0, 1, 2)$ , the squared first derivative of the radial wave-function at the origin  $|R'_{1P}(0)|^2 = 0.075 \text{ GeV}^5$  and the squared radial wave-function at the origin  $|R_{2S}(0)|^2 = 0.529 \text{ GeV}^3$  [33].

### III. NUMERICAL RESULTS AND DISCUSSIONS

To do the numerical calculation, we take  $m_c = 1.5 \text{ GeV}$  and  $\alpha = 1/137$ . The one-loop  $\alpha_s$  running is used, and for each charmonium  $H$ , we set its renormalization and factorization scale as  $\mu_R = \mu_F = M_t = \sqrt{4m_c^2 + (p_t^H)^2}$ <sup>1</sup>. Regarding the feed-down contributions, the resultant  $J/\psi$  transverse momentum can be achieved by a shift,  $p_t^{J/\psi} = \frac{m_{J/\psi}}{m_H} p_t^H$ , where  $m_H$  stands for charmonium mass. The charmonium masses are [31]:  $m_{J/\psi} = 3.097 \text{ GeV}$ ,  $m_{\psi'} = 3.686 \text{ GeV}$ ,  $m_{\chi_{c0}} = 3.415 \text{ GeV}$ ,  $m_{\chi_{c1}} = 3.511 \text{ GeV}$ , and  $m_{\chi_{c2}} = 3.556 \text{ GeV}$ .

$\sqrt{S}$	$\sigma_{3S_1^{[1]}}^{J/\psi}$	$\sigma_{1S_0^{[8]}}^{J/\psi}$	$\sigma_{3S_1^{[8]}}^{J/\psi}$	$\sigma_{3P_1^{[8]}}^{J/\psi}$
250 GeV	$8.00 \times 10^{-4}$	$1.40 \times 10^{-3}$	$3.46 \times 10^{-5}$	$1.94 \times 10^{-2}$
500 GeV	$3.47 \times 10^{-4}$	$1.09 \times 10^{-3}$	$1.62 \times 10^{-5}$	$1.46 \times 10^{-2}$
1000 GeV	$1.36 \times 10^{-4}$	$5.66 \times 10^{-4}$	$6.87 \times 10^{-6}$	$7.60 \times 10^{-3}$

TABLE I. The integrated cross-section (in unit: nb) for the direct  $J/\psi$  photoproduction in association with a  $c\bar{c}$  pair at the ILC.  $|y| < 4.5$ .

We present the integrated cross-section for the  $J/\psi$  photoproduction in association with a  $c\bar{c}$  pair in Tables

$\sqrt{S}$	$\sigma_{\text{direct}}$	$\sigma_{\text{feed-down from } \psi'}$	$\sigma_{\text{feed-down from } \chi_{cJ}}$
250 GeV	$2.16 \times 10^{-2}$	$5.79 \times 10^{-3}$	$6.29 \times 10^{-4}$
500 GeV	$1.60 \times 10^{-2}$	$4.18 \times 10^{-3}$	$4.16 \times 10^{-4}$
1000 GeV	$8.31 \times 10^{-3}$	$2.14 \times 10^{-3}$	$2.07 \times 10^{-4}$

TABLE II. The integrated cross-section (in unit: nb) for the prompt  $J/\psi$  photoproduction in association with a  $c\bar{c}$  pair at the ILC. As for the direct  $J/\psi$  production, the four Fock states' contributions have been summed up.  $|y| < 4.5$ .

I and II. The integrated cross-section decreases with the increment of the  $e^+e^-$  collision energy  $\sqrt{S}$ . The photoproduction of  $J/\psi$  is dominated by direct production, while the feed-down contribution is sizable. More explicitly, when  $\sqrt{S} = 1 \text{ TeV}$ , the direct channel provide  $\sim 78\%$  contribution to the prompt  $J/\psi$  production, that of the feed-down from  $\psi'$  is  $\sim 20\%$ , and that of feed-down from  $\chi_{cJ}$  is  $\sim 2\%$ . Furthermore, for the direct production, the color-octet Fock states' contributions are large, i.e. two Fock states  $J/\psi(^3P_J^{[8]})$  and  $J/\psi(^1S_0^{[8]})$  provide over 95% contribution to the direct  $J/\psi$  cross-section. Thus the future new measurements on  $J/\psi$  photoproduction at the ILC can provide a useful platform for testing the NRQCD color-octet mechanism.

As an important point, we provide an explanation on why  $J/\psi(^1S_0^{[8]})$  and  $J/\psi(^3P_J^{[8]})$  channels provide such large contributions in comparison to the color-singlet case. By analyzing the topologies of Feynman diagrams, it is noted that the largest contributions of  $J/\psi(^1S_0^{[8]})$  and  $J/\psi(^3P_J^{[8]})$  mainly come from Fig.(1.(e)), which is absent for the color-singlet cases due to the color conservation. The squared invariant mass of the internal gluon of Fig.(1.(e)) is,  $k^2 = (p_1 - p_3)^2 = 4m_c^2 - 2p_1 \cdot p_3$  with  $p_1 \cdot p_3 = x \frac{\sqrt{S}}{2} (E_H - p_{3z})$ , where  $E_H (= \frac{e^y + e^{-y}}{2} M_t)$  is the charmonium  $H$  energy,  $p_{3z} (= \frac{e^y - e^{-y}}{2} M_t)$  is the projection of its 3-momentum to the flying direction of the initial photon which attaches to  $H$ , and  $y$  is the rapidity of  $H$ .  $H$  stands for  $J/\psi(^1S_0^{[8]})$  or  $J/\psi(^3P_J^{[8]})$ , and  $x$  is the momentum fraction of this photon to the electron or positron. Then the  $k^2$ -expression can be rewritten as

$$\begin{aligned} k^2 &= 4m_c^2 - x\sqrt{S}M_te^{-y} \\ &= 4m_c^2 - 2(E_H + E_g) \times M_te^{-y} \\ &= -4m_c^2 e^{-2y} - (1 + e^{-2y})(p_t^H)^2 - 2E_g M_t e^{-y}, \end{aligned} \quad (23)$$

where  $E_g$  is the energy of the internal gluon. In small  $p_t$  region, the magnitude of  $k^2$  reduces exponentially with the increment of  $y$  and could be very small, leading to large contributions to the production cross-section.

In addition to the topology, the LBS photon density function provides another important factor for large production cross-sections. A bigger energy  $E_H$  corresponds to a bigger rapidity  $|y|$ , and vice versa. On the other hand, a larger photon momentum fraction  $x$  indicates more  $H$  events with larger energy can be achieved. As shown by Fig.(2), the LBS photon density function be-

<sup>1</sup> Taking  $\mu_R = M_t/2$ , the prompt cross-section shall be increased by 70%, and taking  $\mu_R = 2M_t$ , the prompt cross-section shall be decreased by 30%. Such a large scale error could be suppressed by a high-order calculation and/or a proper scale setting [34].

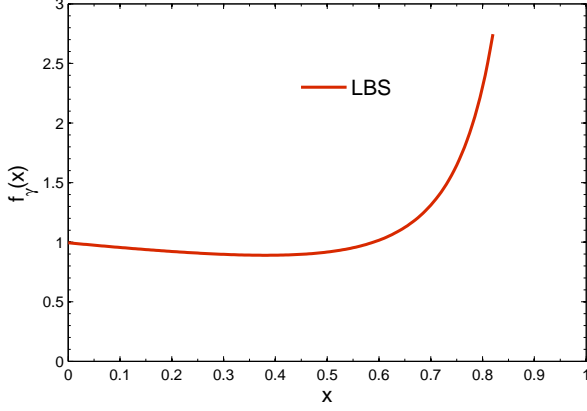


FIG. 2. The LBS photon density function.

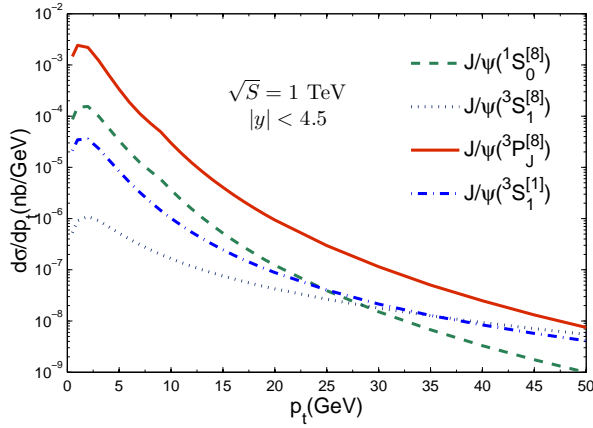


FIG. 3. The  $p_t$ -distributions for the direct  $J/\psi$  production associated with a  $c\bar{c}$  pair at the ILC. The dash-dot, the dashed, the dotted and the solid lines are for  $J/\psi(3S_1^{[1]})$ ,  $J/\psi(1S_0^{[8]})$ ,  $J/\psi(3S_1^{[8]})$  and  $J/\psi(3P_J^{[8]})$ , respectively.

has moderately in small and intermediate  $x$  regions and increases fast when approaching to its allowable largest  $x$ . Thus the contributions of Fig.(1.(e)) will be further enhanced by LBS photons.

We present the  $p_t$ -distributions for the direct and prompt  $J/\psi$  productions associated with a  $c\bar{c}$  pair at the ILC with  $\sqrt{S} = 1$  TeV in Figs.(3, 4). Fig.(3) shows that the color-octet and color-singlet channels have different  $p_t$  behaviors. Fig.(4) shows the relative importance of the feed-down contributions from  $\psi'$  and  $\chi_{cJ}$  to the direct one. It is noted that the  $J/\psi(3P_J^{[8]})$  channel, together with  $J/\psi(1S_0^{[8]})$  channel, provide the dominant contributions to  $J/\psi$  production. In different to other channels, the  $J/\psi(3S_1^{[8]})$  channel scales as  $1/p_t^4$  due to the one gluon fragmentation mechanism. Thus even though its differ-

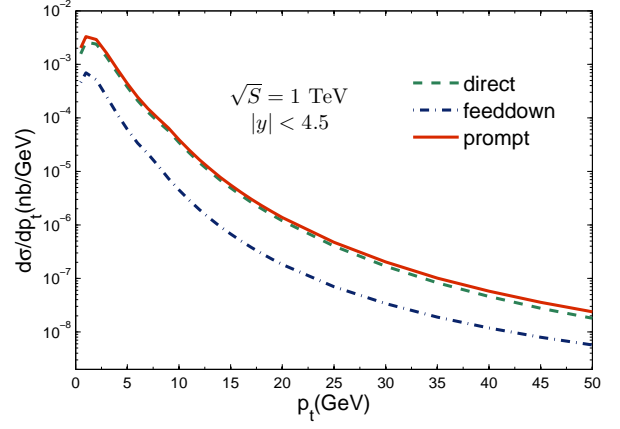


FIG. 4. The  $p_t$ -distributions for the prompt  $J/\psi$  production associated with a  $c\bar{c}$  pair at the ILC. The dashed line is for direct  $J/\psi$  production, in which four Fock states' contributions have been summed up. The dash-dot line is for the feed-down contribution from  $\psi'$  and  $\chi_{cJ}$  decay. The solid line is for the prompt production.

ential cross-section is small in low  $p_t$  region, it becomes important in high  $p_t$  region, i.e.,  $p_t > 50$  GeV.

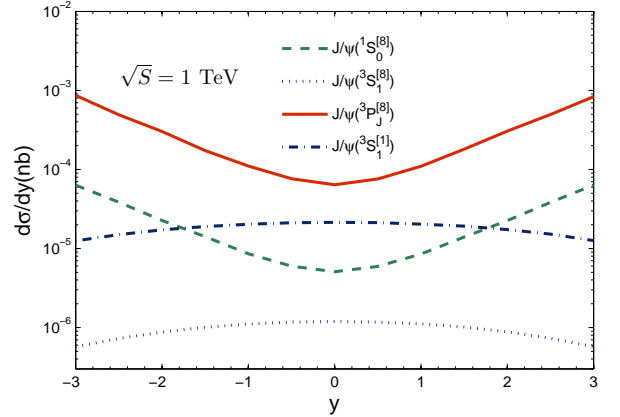


FIG. 5. The  $y$ -distributions for direct  $J/\psi$  production associated with a  $c\bar{c}$  pair at the ILC. The dash-dot, the dashed, the dotted and the solid lines are for  $J/\psi(3S_1^{[1]})$ ,  $J/\psi(1S_0^{[8]})$ ,  $J/\psi(3S_1^{[8]})$  and  $J/\psi(3P_J^{[8]})$ , respectively.

We present the  $y$ -distributions for the direct and prompt  $J/\psi$  productions associated with a  $c\bar{c}$  pair at the ILC with  $\sqrt{S} = 1$  TeV in Figs.(5, 6). Fig.(5) shows that the rapidity distributions of the four Fock states can be divided into two groups, whose behavior is either concave or convex. Those two types of rapidity distributions can be adopted to distinguish the color-octet states from the color-singlet one. The concave behavior of  $J/\psi(1S_0^{[8]})$

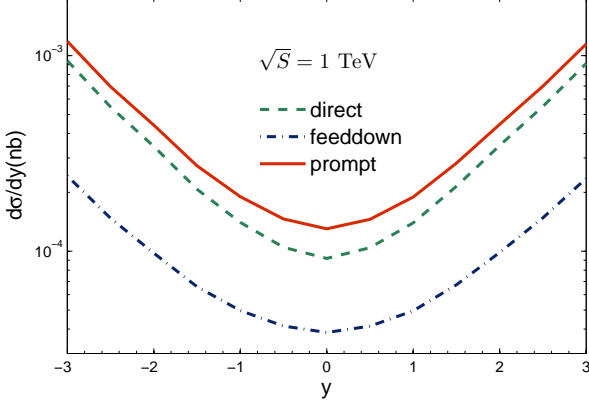


FIG. 6. The  $y$ -distributions for prompt  $J/\psi$  production associated with a  $c\bar{c}$  pair at the ILC. The dashed line is for direct  $J/\psi$  production, in which four Fock states' contributions have been summed up. The dash-dot line is for the feed-down contribution from  $\psi'$  and  $\chi_{cJ}$  decay. The solid line is for the prompt production.

and  $J/\psi(3P_J^{[8]})$  channels is consistent with the explanation (23) for the large cross-section of  $J/\psi(1S_0^{[8]})$  and  $J/\psi(3P_J^{[8]})$ : the largest  $k^2$ -magnitude is achieved at  $y = 0$  which leads to the lowest point of the concave, a larger rapidity leads to a smaller  $k^2$ -magnitude and a larger differential distributions.

Reviewing the long standing  $J/\psi$  polarization puzzle which challenges the NRQCD theory [24], besides the yields, we make a discussion on the polarization of prompt  $J/\psi$  of the process. The polarization observable  $\lambda$  for  $J/\psi$  is defined as [35]

$$\lambda = \frac{d\sigma_{11}^{J/\psi} - d\sigma_{00}^{J/\psi}}{d\sigma_{11}^{J/\psi} + d\sigma_{00}^{J/\psi}}, \quad (24)$$

where  $d\sigma_{S_z S'_z}^{J/\psi}$  ( $S_z, S'_z = 0, \pm 1$ ) is the spin density matrix, which can be calculated by FDC. The feed-down contributions from  $\psi'$  and  $\chi_{cJ}$  are much more involved, detailed procedures for calculating the parameter  $\lambda$  for the prompt  $J/\psi$  can be found in Refs.[35, 36].

We present the polarization parameter  $\lambda$  as a function of  $p_t$  in Fig.(7). As shown by Table II, the direct  $J/\psi$  dominates the production cross-section, so in our analysis, we shall only consider the dominant feed-down contribution from  $\psi'$ . In fact, because the  $\chi_{cJ}$  feed-down contribution to the integrated cross-section is only about 2%, thus its contribution to  $\lambda$  is negligible. It is noted that the  $J/\psi(3S_1^{[1]})$  polarization and the prompt  $J/\psi$  polarization behave quite differently from each other in whole  $p_t$  region. In small  $p_t$  region, the prompt polarization is dominated by  $J/\psi(3P_J^{[8]})$  and is longitudinal. In high  $p_t$  region, it becomes transverse due to the one gluon fragmentation mechanism of  $J/\psi(3S_1^{[8]})$ . Thus, besides the

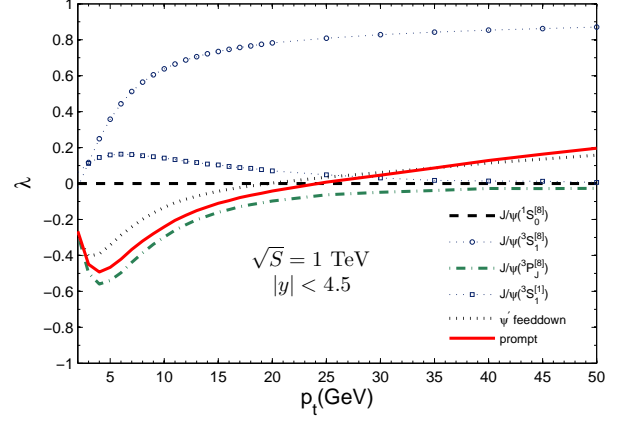


FIG. 7.  $J/\psi$  polarization parameter  $\lambda$  as a function of  $p_t$ . The label 'prompt' represents the sum of the direct and  $\psi'$  feed-down contributions.

aforementioned  $p_t$ - and  $y$ - distributions, the polarization parameter  $\lambda$  can be another useful tool to test the color-octet mechanism.

#### IV. SUMMARY

We have studied the photoproduction of prompt  $J/\psi$  in association with a  $c\bar{c}$  pair within the framework of NRQCD. The color-octet charmonium states, especially  $J/\psi(3P_J^{[8]})$  and  $J/\psi(1S_0^{[8]})$ , provide dominate contributions to the production.

At the ILC with the  $e^+e^-$  collision energy  $\sqrt{S} = 1$  TeV, the color-singlet cross-section  $\sigma_{3S_1^{[1]}}$  is only  $\sim 1.3\%$  of the NRQCD prompt prediction  $\sigma_{\text{NRQCD}}$ <sup>2</sup>, which includes both direct and feed-down contributions. The total feed-down cross-section is sizable, providing  $\sim 22\%$  of  $\sigma_{\text{NRQCD}}$ , thus those feed-down channels should be taken into consideration as a sound prediction. Moreover, the predicted  $J/\psi$   $p_t$ - and  $y$ - distributions, as well as the  $J/\psi$  polarization, given by the color-singlet mechanism and NRQCD are quite different.

If taking the ILC luminosity as  $\mathcal{L} \simeq 10^{34} \text{cm}^{-2} \text{s}^{-1}$ , sizable  $J/\psi$  events can be generated in one operation year, i.e. about  $2.7 \times 10^6$ ,  $2.0 \times 10^6$  or  $1.1 \times 10^6$  events can be generated for  $\sqrt{S} = 250$  GeV, 500 GeV or 1 TeV, respectively. Thus the  $J/\psi$  photoproduction channel shall provide a useful platform for testing the NRQCD color-octet mechanism.

<sup>2</sup> Throughout the paper, we have adopted a conservative rapidity range  $|y| < 4.5$  to do the calculation. If taking a smaller rapidity region as  $|y| < 2.0$ , the percentage of  $\sigma_{3S_1^{[1]}}$  to  $\sigma_{\text{NRQCD}}$  shall be raised up to  $\sim 8.7\%$ .



**Acknowledgments:** We thank Rong Li for helpful discussions. This work was supported in part by the Natural Science Foundation of China under Grant

No.11275280 and No.11405268, and by Fundamental Research Funds for the Central Universities under Grant No.CDJZR305513.

- 
- [1] G. T. Bodwin, E. Braaten and G. P. Lepage, “Rigorous QCD analysis of inclusive annihilation and production of heavy quarkonium,” *Phys. Rev. D* **51**, 1125 (1995) [*Phys. Rev. D* **55**, 5853 (1997)].
  - [2] N. Brambilla *et al.*, “Heavy quarkonium: progress, puzzles, and opportunities,” *Eur. Phys. J. C* **71**, 1534 (2011).
  - [3] N. Brambilla *et al.*, “QCD and Strongly Coupled Gauge Theories: Challenges and Perspectives,” *Eur. Phys. J. C* **74**, 2981 (2014).
  - [4] E. Braaten and S. Fleming, “Color octet fragmentation and the  $\psi'$  surplus at the Tevatron,” *Phys. Rev. Lett.* **74**, 3327 (1995).
  - [5] P. L. Cho and A. K. Leibovich, “Color octet quarkonia production,” *Phys. Rev. D* **53**, 150 (1996).
  - [6] P. L. Cho and A. K. Leibovich, “Color octet quarkonia production. 2.,” *Phys. Rev. D* **53**, 6203 (1996).
  - [7] H. F. Zhang, Z. Sun, W. L. Sang and R. Li, “Impact of  $\eta_c$  hadroproduction data on charmonium production and polarization within NRQCD framework,” *Phys. Rev. Lett.* **114**, 092006 (2015).
  - [8] Z. Sun and H. F. Zhang, “Reconciling charmonium production and polarization data within the nonrelativistic QCD framework,” arXiv:1505.02675 [hep-ph].
  - [9] R. Aaij *et al.* [LHCb Collaboration], *Eur. Phys. J. C* **73**, 2631 (2013).
  - [10] S. Chatrchyan *et al.* [CMS Collaboration], *Phys. Lett. B* **727**, 381 (2013).
  - [11] R. Aaij *et al.* [LHCb Collaboration], *Eur. Phys. J. C* **75**, 311 (2015).
  - [12] K. Abe *et al.* [Belle Collaboration], “Observation of double  $c\bar{c}$  production in  $e^+e^-$  annihilation at  $\sqrt{s}$  approximately 10.6 GeV,” *Phys. Rev. Lett.* **89**, 142001 (2002).
  - [13] R. Aaij *et al.* [LHCb Collaboration], “Observation of double charm production involving open charm in pp collisions at  $\sqrt{s} = 7$  TeV,” *JHEP* **1206**, 141 (2012) [*JHEP* **1403**, 108 (2014)].
  - [14] K. Hagiwara, E. Kou, Z. H. Lin, C. F. Qiao and G. H. Zhu, “Inclusive  $J/\psi$  productions at  $e^+e^-$  colliders,” *Phys. Rev. D* **70**, 034013 (2004).
  - [15] K. Y. Liu, Z. G. He and K. T. Chao, “Inclusive charmonium production via double  $c\bar{c}$  in  $e^+e^-$  annihilation,” *Phys. Rev. D* **69**, 094027 (2004).
  - [16] Y. J. Zhang and K. T. Chao, “Double charm production  $e^+e^- \rightarrow J/\psi + c + \bar{c}$  at B factories with next-to-leading order QCD correction,” *Phys. Rev. Lett.* **98**, 092003 (2007).
  - [17] B. Gong and J. X. Wang, “Next-to-leading-order QCD corrections to  $e^+e^- \rightarrow J/\psi(c\bar{c})$  at the B factories,” *Phys. Rev. D* **80**, 054015 (2009).
  - [18] Z. G. He, Y. Fan and K. T. Chao, “Relativistic corrections to  $J/\psi$  exclusive and inclusive double charm production at B factories,” *Phys. Rev. D* **75**, 074011 (2007).
  - [19] A. V. Berezhnuy, V. V. Kiselev, A. K. Likhoded and A. I. Onishchenko, “Doubly charmed baryon production in hadronic experiments,” *Phys. Rev. D* **57**, 4385 (1998).
  - [20] S. P. Baranov, “Topics in associated  $J/\psi + c + \bar{c}$  production at modern colliders,” *Phys. Rev. D* **73**, 074021 (2006).
  - [21] J. P. Lansberg, “On the mechanisms of heavy-quarkonium hadroproduction,” *Eur. Phys. J. C* **61**, 693 (2009).
  - [22] Z. Sun, X. G. Wu, G. Chen, J. Jiang and Z. Yang, “Heavy quarkonium production through the semi-exclusive  $e^+e^-$  annihilation channels round the  $Z^0$  peak,” *Phys. Rev. D* **87**, 114008 (2013).
  - [23] G. Aarons *et al.* [ILC Collaboration], “International Linear Collider Reference Design Report Volume 2: Physics at the ILC,” arXiv:0709.1893 [hep-ph].
  - [24] T. Affolder *et al.* [CDF Collaboration], *Phys. Rev. Lett.* **85**, 2886 (2000).
  - [25] J. X. Wang, “Progress in FDC project,” *Nucl. Instrum. Meth. A* **534**, 241 (2004).
  - [26] I. F. Ginzburg, G. L. Kotkin, V. G. Serbo, and V. I. Telnov, *Nucl. Instrum. Meth.* **205**, 47 (1983).
  - [27] J. P. Ma, B. H. J. McKellar and C. B. Paranjit, “ $J/\psi$  production at photon - photon colliders as a probe of the color octet mechanism,” *Phys. Rev. D* **57**, 606 (1998).
  - [28] R. Li and K. T. Chao, “Photoproduction of  $J/\psi$  in association with a  $c\bar{c}$  pair,” *Phys. Rev. D* **79**, 114020 (2009).
  - [29] C. F. Qiao and J. X. Wang, “ $J/\psi + c + \bar{c}$  photoproduction in  $e^+e^-$  scattering,” *Phys. Rev. D* **69**, 014015 (2004).
  - [30] V. I. Telnov, “Problems of Obtaining  $\gamma\gamma$  and  $\gamma e$  Colliding Beams at Linear Colliders,” *Nucl. Instrum. Meth. A* **294**, 72 (1990).
  - [31] K. A. Olive *et al.* [Particle Data Group Collaboration], *Chin. Phys. C* **38**, 090001 (2014).
  - [32] L. Jia, L. Yu and H. F. Zhang, “A global analysis of the experimental data on  $\chi_c$  meson hadroproduction,” arXiv:1410.4032 [hep-ph].
  - [33] E. J. Eichten and C. Quigg, “Quarkonium wave functions at the origin,” *Phys. Rev. D* **52**, 1726 (1995).
  - [34] X. G. Wu, S. J. Brodsky and M. Mojaza, “The Renormalization Scale-Setting Problem in QCD,” *Prog. Part. Nucl. Phys.* **72**, 44 (2013).
  - [35] M. Beneke, M. Kramer and M. Vanttinen, “Inelastic photoproduction of polarized  $J/\psi$ ,” *Phys. Rev. D* **57** (1998) 4258.
  - [36] B. Gong, L. P. Wan, J. X. Wang and H. F. Zhang, “Polarization for Prompt  $J/\psi$  and  $\psi'$  Production at the Tevatron and LHC,” *Phys. Rev. Lett.* **110**, 042002 (2013).